ATLAS NOTE

ATL-PHYS-PUB-2016-021

30th September 2016

Prospects for a search for direct stau production in events with at least two hadronic taus and missing transverse momentum at the High Luminosity LHC with the ATLAS Detector

The ATLAS Collaboration

Abstract

Only one scenario of combined $\tilde{\tau}_L\tilde{\tau}_L$ and $\tilde{\tau}_R\tilde{\tau}_R$ production is excluded from the current searches at LHC, where the $\tilde{\tau}_R$ mass is 109 GeV and the $\tilde{\chi}_1^0$ is massless. The reach at the high-luminosity phase of the LHC is expected to significantly extend beyond the current limits. This document presents example benchmark studies for direct stau production in events with at least two hadronic taus and missing transverse momentum with a parameterised simulation of the ATLAS detector at a centre-of-mass energy of 14 TeV. Results are shown for an integrated luminosity of 3000 fb^{-1}. For a massless $\tilde{\chi}_1^0$, the 5σ discovery sensitivity reaches up to 100 (120) to 500 (430) GeV in $\tilde{\tau}$ mass for the combined $\tilde{\tau}_L\tilde{\tau}_L$ and $\tilde{\tau}_R\tilde{\tau}_R$ (pure $\tilde{\tau}_L\tilde{\tau}_L$) production, and the 95 % CL exclusion contour reaches 700 GeV in $\tilde{\tau}$ mass for the combined $\tilde{\tau}_L\tilde{\tau}_L$ and $\tilde{\tau}_R\tilde{\tau}_R$ production, 650 (540) GeV for pure $\tilde{\tau}_L\tilde{\tau}_L$ (pure $\tilde{\tau}_R\tilde{\tau}_R$) production with massless $\tilde{\chi}_1^0$.

ATL-PHYS-PUB-2016-021
01 October 2016

1 Introduction

Supersymmetry (SUSY) [1–6] proposes for every boson (fermion) of the Standard Model (SM) there exists a fermionic (bosonic) partner. The existence of SUSY particles with masses at the electroweak scale leads to contributions that can cancel quadratic divergences to the Higgs mass corrections. SUSY can also accommodate the unification of the gauge interactions and a radiative breaking of the electroweak symmetry. Under the conservation of R-parity [7], the lightest SUSY particle (LSP) is stable and is an excellent candidate to account for the dark matter in the universe. Furthermore, the minimal supersymmetric model (MSSM) requires a Higgs boson with mass below ~135 GeV which could be consistent with the recently observed Higgs-like resonance [8, 9]. The discovery (or exclusion) of weak-scale SUSY is one of the highest physics priorities for the current and future LHC, including the high luminosity upgrade, HL-LHC ($\sqrt{s}$ =14 TeV; 3000 fb^{-1}). The multi-TeV energy range probed with the LHC and the HL-LHC will not be accessible at any other current facility.

In many SUSY scenarios with large $\tan\beta$, the stau ($\tilde{\tau}$) is lighter than the selectron and smuon [10], resulting in tau-rich final states. Co-annihilation processes favor a light $\tilde{\tau}$ that has a small mass splitting with a bino LSP, as it can set the relic density to the observed value [11–14]. Light staus are attractive since they can affect the decay rate of the Higgs into di-photons [15] and light sleptons can explain the g-2 discrepancy [16]. This note shows results of the discovery and exclusion reach of ~3000 fb^{-1} at the HL-LHC, with $\sqrt{s}$=14 TeV pp collisions for direct stau production in events with at least two hadronic taus and missing transverse momentum assuming R-parity conserving SUSY.

1.1 The LHC and HL-LHC

In 2012, the LHC delivered 22.8 fb^{-1} of proton-proton collisions at a centre-of-mass-energy of 8 TeV. During the shutdown following the end of data-taking (LS1), the machine has been consolidated to be able to operate at a centre-of-mass-energy of 13 TeV, with the possibility of future 14 TeV collisions. The 13 TeV data taking started from 2015, in this period the LHC will collect ~100 fb^{-1}. A second long shutdown (LS2) will follow, during which the injection chain is foreseen to be modified to allow for instantaneous luminosities up to ~2×10^{34} cm^{-2}s^{-1}. The maximum average number of proton-proton collisions per bunch crossing is expected to be $\langle\mu\rangle \sim 60$ and the data collected up to the next long shutdown (LS3) will amount to ~300 fb^{-1}. During LS3, the accelerator is foreseen to be upgraded to the HL-LHC which will be able to achieve luminosities of ~7×10^{34} cm^{-2}s^{-1}. The HL-LHC is expected to deliver an average number of pile up events per bunch crossing of $\langle\mu\rangle \sim 200$ and the data collected will amount to ~3000 fb^{-1}. The increased pile up degrades the ability to reconstruct quantities like missing transverse momentum and therefore event numbers do not scale simply with integrated luminosity.

1.2 The ATLAS experiment

ATLAS [17] is a multipurpose particle physics detector with a forward-backward symmetric cylindrical geometry and nearly 4π coverage in solid angle[1]. The layout of the detector is dominated by four superconducting magnet systems, which comprise a thin solenoid surrounding inner tracking detectors

[1] ATLAS uses a right-handed coordinate system with its origin at the nominal interaction point in the centre of the detector and the z-axis along the beam pipe. Cylindrical coordinates (r, ϕ) are used in the transverse plane, ϕ being the azimuthal angle around the beam pipe. The pseudorapidity η is defined in terms of the polar angle θ by $\eta = -\ln\tan(\theta/2)$.

(ID) with $|\eta| < 2.5$ and three large toroids supporting a large muon tracker (MS). The MS covers a range of $|\eta| < 2.7$ for precision measurements and $|\eta| < 2.4$ for triggering purposes. In the pseudorapidity region $|\eta| < 3.2$, high-granularity liquid-argon (LAr) electromagnetic (EM) sampling calorimeters surround the solenoid magnet. An iron-scintillator tile calorimeter provides hadronic coverage over $|\eta| < 1.7$. The end-cap and forward regions, spanning $1.5 < |\eta| < 4.9$, are instrumented with LAr calorimeters for both EM and hadronic measurements. Upgrades to the detector and the triggering system are planned to adapt the experiment to the increasing instantaneous and integrated luminosity expected with the HL-LHC [18].

2 Searches for *R*-parity conserving SUSY

2.1 SUSY searches at the LHC

In the framework of generic R-parity conserving supersymmetric extensions of the SM, SUSY particles are produced in pairs and the LSP is stable. In a large fraction of the parameter space, the LSP is the lightest neutralino, where neutralinos ($\tilde{\chi}_j^0$, $j = 1, 2, 3, 4$) and charginos ($\tilde{\chi}_i^{\pm}$, $i = 1, 2$) are the mass eigenstates originating from the superposition of the SUSY partners of Higgs and electroweak gauge bosons (higgsinos and electroweak gauginos). The scalar partners of right-handed and left-handed fermions can mix to form two mass eigenstates, nearly degenerate in the case of first and second generation squarks and sleptons ($\tilde{q}$ and $\tilde{l}$), whilst possibly split in the case of bottom and top squarks (sbottom, $\tilde{b}$ and stop, $\tilde{t}$) and tau sleptons (stau, $\tilde{\tau}$).

The ATLAS Collaboration is currently carrying out a broad programme of searches [19–21] including searches for light-flavour squarks and gluinos, weakly produced sparticles, and third generation squarks using data taken in 2012 at a centre-of-mass-energy of 8 TeV. The first results from run2 using data taken in 2015 at a centre-of-mass-energy of 13 TeV are becoming available and excluded gluino masses below 1400 GeV [22], under the assumption of a simplified model and a very light LSP. In particular, for the search described in this document, the current observed 95% CL limits exclude the scenario with $\tilde{\tau}_R$ mass 109 GeV under the assumption of a massless LSP [21].

2.2 SUSY searches at the HL-LHC

Previous studies of the discovery and exclusion reach of the HL-LHC have been carried out for squark and gluino production, for the production of top and bottom squarks and for the production of charginos and neutralinos [23, 24]. This note updates the searches for direct stau production in events with at least two hadronic taus and missing transverse momentum, with parameterisations of the upgraded ATLAS detector configurations and re-optimised selections, under the assumptions of 3000 fb^{-1} at $\sqrt{s}$= 14 TeV and $\langle\mu\rangle \sim 200$ (HL-LHC).

For these analyses, Monte Carlo (MC) generator level information is used for both the background and the signal processes. The detector response is a parameterisation of the upgraded ATLAS detector performance based on Monte Carlo samples using full simulation of the upgraded detector in high pile-up conditions, as described in Refs. [25]. The parameterisations describe the resolution and the reconstruction efficiencies of electrons, muons, taus, jets, b-jets and missing transverse momentum. The mis-identification of c-jets and light flavour jets as b-jets is accounted for in the parameterisations. The parameterised response functions account for the effect of the number of interactions per bunch crossing

of 200 with 25ns bunch spacing. According to the parameterisations, the effect of the trigger is considered by applying the efficiencies of 80% on leading and sub-leading taus with a minumum p_{T} of 50 and 40 GeV respectively. The $di\text{-}\tau + E_{\mathrm{T}}^{\mathrm{miss}}$ trigger or $di\text{-}\tau + \Delta R$ trigger will be used at the HL-LHC.

2.3 Monte Carlo Samples

Several Monte Carlo generators are used to model the dominant SM processes and new physics signals relevant for the analyses. The $W^{(*)}$+jets process is simulated by Alpgen [26] + Pythia with Perugia2011C tune and the parton distribution functions (PDFs) set CTEQ6L1 [27]. The top quark pair-production contribution is generated using Powheg +Pythia with Perugia2011C tune. Sherpa is used to simulate $Z^{(*)}$+jets process, and PDF set CT10. The vector boson pair production processes are generated using Alpgen + Jimmy ($W^{(*)}Z^{(*)}$ and $Z^{(*)}Z^{(*)}$) with the PDF set CTEQ6L1 and up to 3 jets in the ME+PS, and Powheg [28]+Pythia 8 ($W^{(*)}W^{(*)}$), in which the CT10 PDF set is used in the matrix element in Powheg, and the A14 [29] tune is used together with the CTEQ6L1 PDF set in Pythia 8.

The signal MC samples are produced with Herwig++ 2.6.3 [30]. They are parametrized as function of the stau and neutralino LSP mass, where the stau mass is bounded from below by the LEP limit [31–34], and the neutralino mass is bounded from above by the stau mass. The mixing matrix for the scalar taus is antidiagonal such that the $\tilde{\tau}_1$ is right-handed and the $\tilde{\tau}_2$ is left-handed and no mixed production modes ($\tilde{\tau}_1\tilde{\tau}_2$) are expected. The masses of $\tilde{\tau}_1$ and $\tilde{\tau}_2$ are equal. We here set $m(\tilde{\tau}_{1,2})$ directly rather than fixing $m(\tilde{\tau}_{L,R})$ and computing $m(\tilde{\tau}_{1,2})$ as in the pMSSM-inspired approach used for the grids in [21]. The event kinematics for $\tilde{\tau}_1$ and $\tilde{\tau}_2$ are assumed to be the same, thus no separate optimization is attempted. The event yields are normalised to the NLO+NLL cross sections, which have been calculated with Resummino 1.0.6 [35], using the NLO CT10 PDF set.

3 Search for the direct production of staus

If charginos and next-to-lightest neutralinos are too heavy to be produced at the LHC, direct production of stau pairs [36] might become the dominant electroweak production process in the pMSSM. Two simplified models describing the direct production of $\tilde{\tau}^+\tilde{\tau}^-$ are used in this document: one considers stau partners of the left-handed τ lepton ($\tilde{\tau}_{\mathrm{L}}$), and a second considers stau partners of the right-handed τ lepton ($\tilde{\tau}_{\mathrm{R}}$). In both models, the stau decays with a branching fraction of 100% to the SM tau-lepton and the LSP. Next-to-leading order cross-sections for the stau pair production at the LHC as a function of the stau mass are shown in Fig. 1, and the relevant diagram for this model can be seen in Fig. 2. Besides that, the combined production of $\tilde{\tau}_{\mathrm{L}}\tilde{\tau}_{\mathrm{L}}$ and $\tilde{\tau}_{\mathrm{R}}\tilde{\tau}_{\mathrm{R}}$ is also studied in this document.

The main signatures of the studied final states are: two hadronically decaying taus, low jet activity, and large $E_{\mathrm{T}}^{\mathrm{miss}}$ from the neutralinos and neutrinos. The expected background is dominated by W+jets and ttbar.

3.1 Signal Region Selection

The event preselection is based on that of the 8 TeV analysis documented in Ref. [37]. Hadronically decaying taus are selected with p_{T} larger than 20 GeV and $|\eta| < 2.47$, while the p_{T} of the leading (sub-leading) tau is larger than 50 (40) GeV. Leptons are selected with p_{T} larger than 10 GeV and $|\eta| < 2.47$

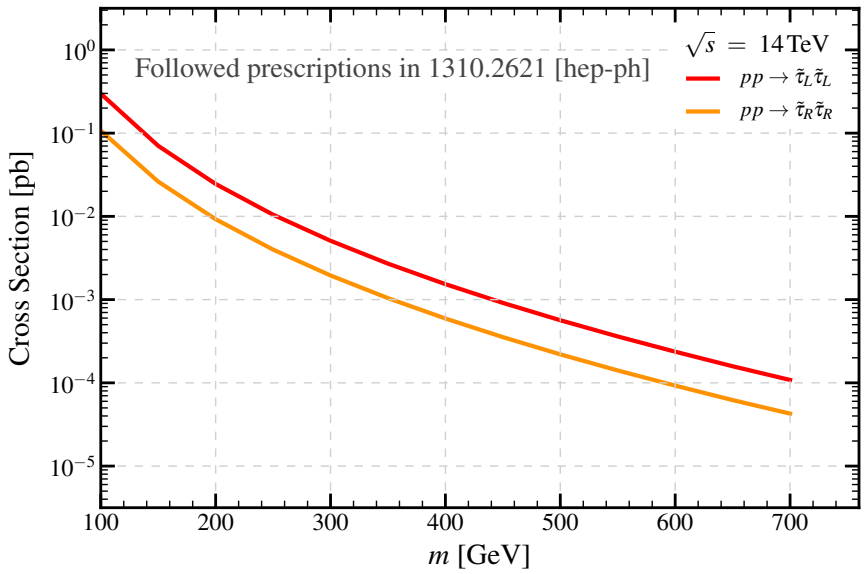

Figure 1: Next-to-leading order cross-sections for the direct stau pair production at the LHC as a function of the stau mass. The left-handed and right-handed stau-pair production cross sections are shown separately.

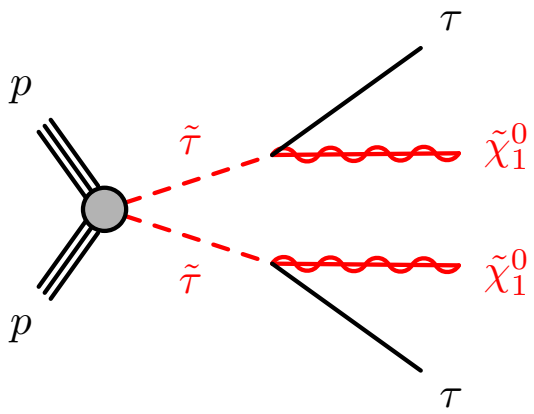

Figure 2: Representative diagram illustrating the pair production of charged staus and subsequent decay into a two-tau final state.

(2.4) for electrons (muons). Jets are reconstructed with the anti-k_t algorithm [38, 39] with a radius parameter of 0.4, with $p_{\mathrm{T}} > 50$ GeV and $|\eta| < 2.5$. To remove close-by objects from one another, an overlap removal based on $\Delta R \equiv \sqrt{(\Delta\phi)^2 + (\Delta\eta)^2}$ is applied. Taus are required to be separated from candidate electrons and muons by $\Delta R(e/\mu, \tau) > 0.2$, otherwise the taus will be discarded. Similarly, jets are required to be separated from candidate electrons and taus by $\Delta R(e/\tau, jet) > 0.2$.

Jets misidentified as taus are parameterised as a function of the jet p_{T} and η, and every jet is assigned a weight corresponding to the tau fake rate. To maximise the available MC statistics, the probability for an event to have one, two or three fake taus is assessed using all possible combinations of jets. Each event is then weighted by the probability it will contribute to the fake tau background. Cases with more than three fake taus are not considered due to the negligible probability (less than 10^{-6}). The truth $E_{\mathrm{T}}^{\mathrm{miss}}$ is computed

as the vectorial sum of the momenta of neutral weakly-interacting particles (neutrinos and neutralinos). It is then smeared to simulate detector response, with a function parameterised in μ and the scalar sum of energy in the calorimeter $\sum E_{\mathrm{T}}$.

Before the optimization, some pre-selection cuts are applied to suppress the SM backgrounds. Events are selected with at least two hadronic taus with opposite sign (OS). All events with electrons and muons are vetoed. A loose jet-veto (rejecting events with jets with $p_{\mathrm{T}} > 60$ GeV) is applied, to reduce the contamination coming from SM backgrounds. The jet veto is safe against pileup because the p_{T} threshold is high. Since the final state contains two $\tilde{\chi}_1^0$, the resulting $E_{\mathrm{T}}^{\mathrm{miss}}$ spectrum tends to be harder than the major SM backgrounds, a 280 GeV cut on the smeared event $E_{\mathrm{T}}^{\mathrm{miss}}$ is applied.

Furthermore, the invariant mass computed from the leading and sub-leading taus after above cut is required to be larger than 100 GeV to reject tau pairs decaying from Z boson. This cut is very efficient to suppress Z+jets and diboson backgrounds, and does not have a big impact on the signal (see Fig. 3). This requirement is referred to as the "Z-veto".

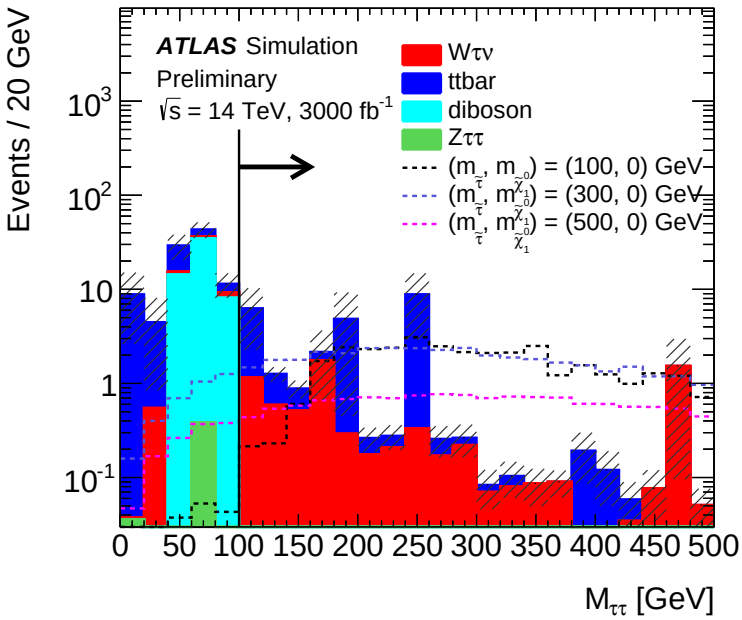

Figure 3: Distribution of the invariant mass of the two leading taus after 2 OS taus, electron and muon veto, loose jet-veto and $E_{\mathrm{T}}^{\mathrm{miss}}$ >280 GeV. The stacked histograms show the expected SM backgrounds normalised to 3000 fb^{-1}. The hatched bands represent the statistical uncertainties on the total SM background. For illustration, the distributions of three SUSY reference points are also shown as dashed lines.

Starting from this common pre-selection, a cut-and-count method is used to define the signal region (SR). Several variables with good discrimination power between signal and SM backgrounds are used: the event $E_{\mathrm{T}}^{\mathrm{miss}}$, $\Delta R(\tau 1, \tau 2)$, which is the angular separation between the leading and next-to-leading tau, $m_{\mathrm{T}\tau 1} + m_{\mathrm{T}\tau 2}$, where $m_{\mathrm{T}\tau 1}$ ($m_{\mathrm{T}\tau 2}$) is the transverse mass computed from the transverse momentum of the leading (next-to-leading) tau and $E_{\mathrm{T}}^{\mathrm{miss}}$, and the "stransverse mass" m_{T2} defined as:

$$m_{\mathrm{T2}} = \min_{\vec{q}_{\mathrm{T}}} \left[\max \left(m_{\mathrm{T}}(\vec{p}_{\mathrm{T}}^{\,\tau 1}, \vec{q}_{\mathrm{T}}), m_{\mathrm{T}}(\vec{p}_{\mathrm{T}}^{\,\tau 2}, E_{\mathrm{T}}^{\mathrm{miss}} - \vec{q}_{\mathrm{T}}) \right) \right], \tag{1}$$

where $\vec{p}_{\mathrm{T}}^{\,\tau 1}$ and $\vec{p}_{\mathrm{T}}^{\,\tau 2}$ are the transverse momenta of the two taus, and $\vec{q}_{\mathrm{T}}$ is a transverse vector that minimises the larger of the two transverse masses m_{T}. The latter is defined by

$$m_{\mathrm{T}}(\vec{p}_{\mathrm{T}}, \vec{q}_{\mathrm{T}}) = \sqrt{2(p_{\mathrm{T}} q_{\mathrm{T}} - \vec{p}_{\mathrm{T}} \cdot \vec{q}_{\mathrm{T}})}. \tag{2}$$

The m_{T2} distribution has a kinematic endpoint for events where two massive pair-produced particles each decay to two particles, one of which is detected (the tau in our case) and the other escapes undetected (the neutralino) [40, 41]. In events with more than two taus, m_{T2} is calculated using all possible tau pairs and the largest value is chosen.

The selections of these variables are optimised for high discovery Z_N [42], defined to be

$$Z_n = \sqrt{2}\,\mathrm{erf}^{-1}\,(1 - 2p) \tag{3}$$

where

$$p \propto \int_0^\infty db\, G(b; N_b, \delta b) \sum_{i=N_{data}}^{\infty} \frac{e^{-b} b^i}{i!} \tag{4}$$

is the probability that the background N_b with uncertainty given by δb fluctuates to N_{data} or above [43]. A systematic uncertainty of 30% on the estimated sum of all backgrounds is assumed, which is consistent with the uncertainties found in published searches [37]. The multi-jet background is largely suppressed by the high $E_{\mathrm{T}}^{\mathrm{miss}}$ cut used in this study so it is not taken into account for the signal region optimisation.

A signal region is defined based on the optimisation results. The selection criteria are shown in Table 1, the distribution of $m_{\mathrm{T}\tau 1} + m_{\mathrm{T}\tau 2}$ before the last cut is shown in Fig. 4.

SR Definition
≥ 2 OS taus
loose jet-veto
Z-veto
$\Delta R(\tau 1, \tau 2) < 3.5$
$E_{\mathrm{T}}^{\mathrm{miss}} > 280$ GeV
$m_{\mathrm{T2}} > 40$ GeV
$m_{\mathrm{T}\tau 1} + m_{\mathrm{T}\tau 2} > 480$ GeV

Table 1: Summary of selection requirements for the direct stau signal region.

3.2 Expected Sensitivity

Limits are set using Z_N: the value of Z_N is required to be larger than 5 for discovery and larger than 1.64 for 95% confidence level (CL) exclusion [2].

[2] A one sided confidence interval is used. Comparing the used prescription with a dedicated 95%CL exclusion test yields very similar results.

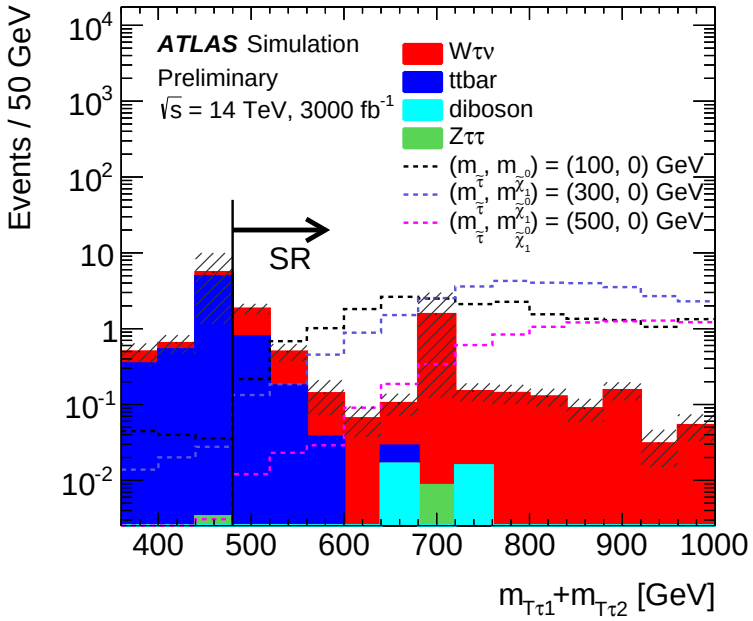

Figure 4: $m_{\mathrm{T}\tau 1} + m_{\mathrm{T}\tau 2}$ distribution in the SR described in Table 1 except for the last cut. The stacked histograms show the expected SM backgrounds normalised to 3000 fb^{-1}. The hatched bands represent the statistical uncertainties on the total SM background. For illustration, the distributions of three SUSY reference points are also shown as dashed lines.

The same systematic uncertainty on the SM backgrounds of 30% used for SR optimisation is assumed. Theoretical uncertainties on the SUSY signal have very small effects on the limits for direct stau pair production. Experimental uncertainties on the SUSY yields have not been considered.

Table 2 shows the expected number of events for the SM backgrounds and three SUSY reference points in the signal region for an integrated luminosity of 3000 fb^{-1}. The SM background is dominated by W+jets production, followed by contributions from $t\bar{t}$ production.

SM process	Event yields
W+jets	1.91 ± 0.19
$t\bar{t}$	0.97 ± 0.23
Z+jets	0.009 ± 0.009
diboson	0.03 ± 0.02
SM total	2.9 ± 0.3
$m(\tilde{\tau}) = 100$ GeV, $m(\tilde{\chi}_1^0) = 0$ GeV	19.1 ± 0.9
$m(\tilde{\tau}) = 300$ GeV, $m(\tilde{\chi}_1^0) = 0$ GeV	31.6 ± 0.4
$m(\tilde{\tau}) = 500$ GeV, $m(\tilde{\chi}_1^0) = 0$ GeV	14.21 ± 0.11

Table 2: Expected numbers of events in the signal region for 3000 fb^{-1}. The shown uncertainties are statistical uncertainties. Expected event yields for three SUSY reference points are also shown.

The 95% CL exclusion limits and 5σ discovery contours on the combined $\tilde{\tau}_{\mathrm{L}}\tilde{\tau}_{\mathrm{L}}$ and $\tilde{\tau}_{\mathrm{R}}\tilde{\tau}_{\mathrm{R}}$ production is

shown in Figure 5. Additional checks with systematic uncertainties of 20% and 50% on SM backgrounds are also shown. There is no significant effect from the change of the systematic uncertainty on SM backgrounds. The sensitivity from pure $\tilde{\tau}_L\tilde{\tau}_L$ or $\tilde{\tau}_R\tilde{\tau}_R$ production and the combination are shown in Fig. 6. Under the assumption of 30% total systematic uncertainty, the 95% CL exclusion contour reaches 700 GeV in $\tilde{\tau}$ mass for the combined $\tilde{\tau}_L\tilde{\tau}_L$ and $\tilde{\tau}_R\tilde{\tau}_R$ production, 650 (540) GeV for pure $\tilde{\tau}_L\tilde{\tau}_L$ (pure $\tilde{\tau}_R\tilde{\tau}_R$) production with massless $\tilde{\chi}_1^0$ The discovery sensitivity reaches 500 (430) GeV in $\tilde{\tau}$ mass for the combined $\tilde{\tau}_L\tilde{\tau}_L$ and $\tilde{\tau}_R\tilde{\tau}_R$ (pure $\tilde{\tau}_L\tilde{\tau}_L$) production with a massless $\tilde{\chi}_1^0$. No discovery sensitivity is found for pure $\tilde{\tau}_R\tilde{\tau}_R$ production due to the too small production cross section.

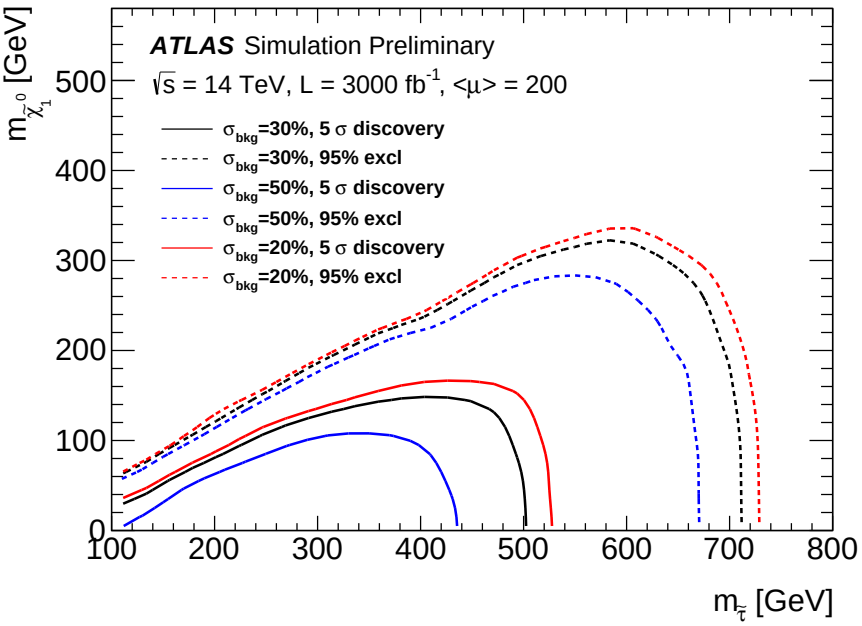

Figure 5: The 95% CL exclusion limits and 5σ discovery contours for 3000 fb^{-1} luminosity on the combined $\tilde{\tau}_L\tilde{\tau}_L$ and $\tilde{\tau}_R\tilde{\tau}_R$ production in HL-LHC with different systematic uncertainties assumption on SM backgrounds. Only one scenario of combined $\tilde{\tau}_L\tilde{\tau}_L$ and $\tilde{\tau}_R\tilde{\tau}_R$ production is excluded from the current searches at LHC, where the $\tilde{\tau}$ ($\tilde{\tau}_R$) mass is 100 (109) GeV and the $\tilde{\chi}_1^0$ is massless [21].

4 Conclusions

The sensitivity to heavy SUSY particles will be increased significantly when the centre-of-mass-energy of the LHC reaches a value close to the design of $\sqrt{s} = 14$ TeV and an integrated luminosity of 3000 fb^{-1}. Feasibility studies on benchmark SUSY scenarios for direct stau pair production are carried out with 14 TeV MC samples and by applying detector response corrections to generator level particles, the 95% CL exclusion and 5σ discovery contours with the assumption of different systematic uncertainties are given, the exclusion limit reaches 700 GeV in $\tilde{\tau}$ mass for the combined $\tilde{\tau}_L\tilde{\tau}_L$ and $\tilde{\tau}_R\tilde{\tau}_R$ production, 650 (540) GeV for pure $\tilde{\tau}_L\tilde{\tau}_L$ (pure $\tilde{\tau}_R\tilde{\tau}_R$) production with massless $\tilde{\chi}_1^0$, and the discovery sensitivity reaches 100 (120) to 500 (430) GeV in $\tilde{\tau}$ mass for the combined $\tilde{\tau}_L\tilde{\tau}_L$ and $\tilde{\tau}_R\tilde{\tau}_R$ (pure $\tilde{\tau}_L\tilde{\tau}_L$) production with a massless $\tilde{\chi}_1^0$ with 30% systematic uncertainty. No discovery sensitivity is found for pure $\tilde{\tau}_R\tilde{\tau}_R$ production due to the too small production cross section.

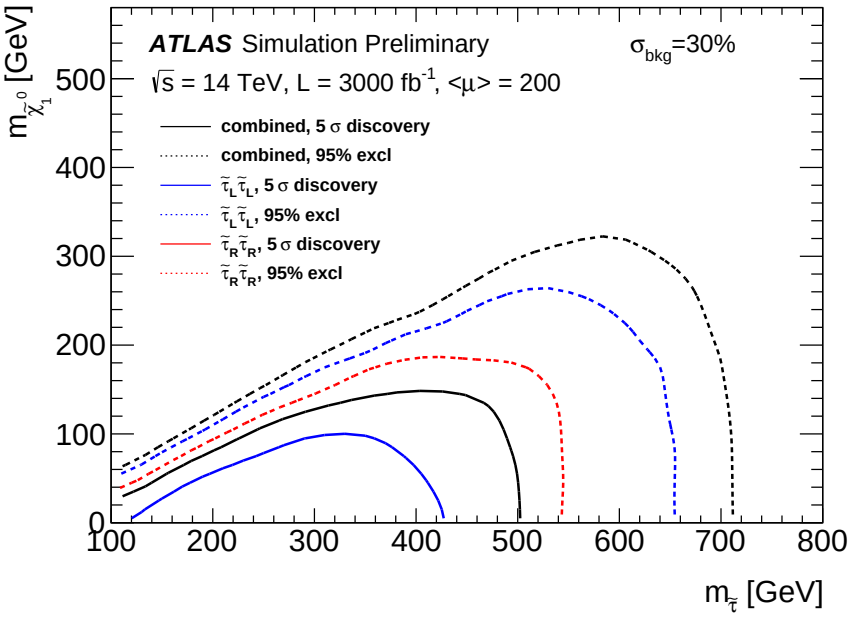

Figure 6: The 95% CL exclusion limits and 5σ discovery contours for 3000 fb^{-1} luminosity on the pure $\tilde{\tau}_L\tilde{\tau}_L$, pure $\tilde{\tau}_R\tilde{\tau}_R$ and combined production in HL-LHC with 30% systematic uncertainty on SM backgrounds.

References

[1] Y. Golfand, E. Likhtman, JETP Lett. **13** (1971) 323.

[2] D. Volkov, V. Akulov, Phys. Lett. **B 46** (1973) 109.

[3] J. Wess, B. Zumino, Nucl. Phys. **B 70** (1974) 39.

[4] J. Wess and B. Zumino, Nucl. Phys. B **78** (1974) 1.

[5] S. Ferrara and B. Zumino, Nucl. Phys. B **79** (1974) 413.

[6] A. Salam and J. A. Strathdee, Phys. Lett. B **51** (1974) 353–355.

[7] G. R. Farrar and P. Fayet, Phys. Lett. B **76** (1978) 575–579.

[8] ATLAS Collaboration, Phys.Lett. **B716** (2012) 1–29, arXiv:1207.7214.

[9] CMS Collaboration, Phys. Lett. B (2012) 30, arXiv:1207.7235.

[10] A. G. Delannoy et al., arXiv:1308.0355 [hep-ph].

[11] K. Griest and D. Seckel, Phys. Rev. **D43** (1991) 3191–3203.

[12] G. Hinshaw et al., Astrophys. J. Suppl. **208** (2013) 19.

[13] V. Khotilovich et al., Phys. Let. **B 618** (2005) 182–192.

[14] J. Ellis et al., Astroparticle Physics **13** (2000) 181–213.

[15] Marcela Carena and others, JHEP **08** (2013) 087, arXiv:1303.4414 [hep-ph].

[16] S. Heinemeyer and others, Physics Reports **425** (2006) 265–368.

[17] ATLAS Collaboration, JINST **3** (2008) S08003.

[18] ATLAS, CERN-LHCC-2012-022. LHCC-I-023 (2012). https://cds.cern.ch/record/1502664.

[19] ATLAS Collaboration, JHEP **10** (2015) 054, arXiv:1507.05525 [hep-ph].

[20] ATLAS Collaboration, Eur. Phys. J. **C 75** (2015) 510, arXiv:1506.08616 [hep-ph].

[21] ATLAS Collaboration, Phys. Rev. **D 93** (2016) 052002, arXiv:1509.07152 [hep-ph].

[22] ATLAS Collaboration, arXiv:1602.061946.

[23] ATLAS Collaboration, ATL-PHYS-PUB-2013-002.

[24] ATLAS Collaboration, ATL-PHYS-PUB-2014-010.

[25] ATLAS Collaboration, CERN-LHCC-2015-020.

[26] M. Mangano *et al.*, JHEP **07** (2003) 001, arXiv:hep-ph/0206293.

[27] J. Pumplin *et al.*, JHEP **0207** (012) 2002, arXiv:0802.0007.

[28] P. Nason, JHEP **0411** (2004) 040, arXiv:hep-ph/0409146.

[29] ATLAS Collaboration,. http://cdsweb.cern.ch/record/1966419.

[30] M. Bahr et al., Eur. Phys. J. **C58** (2008) 639–707, arXiv:0803.0883 [hep-ph].

[31] LEP SUSY Working Group (ALEPH, DELPHI, L3, OPAL),. Notes LEPSUSYWG/01-03.1, 04-01.1, http://lepsusy.web.cern.ch/lepsusy/Welcome.html.

[32] DELPHI Collaboration, J. Abdallah et al., Eur. Phys. J. **C 31** (2003) 421, arXiv:hep-ex/0311019 [hep-ex].

[33] L3 Collaboration, M. Acciarri et al., Phys. Lett. **B 472** (2000) 420, arXiv:hep-ex/9910007 [hep-ex].

[34] OPAL Collaboration, G. Abbiendi et al., Eur. Phys. J. **C 35** (2004) 1, arXiv:hep-ex/0401026 [hep-ex].

[35] B. Fuks, M. Klasen, D. R. Lamprea, and M. Rothering, JHEP **01** (2014) 168, arXiv:1310.2621 [hep-ph].

[36] H. Baer, C. Chen, F. Paige, and X. Tata, Phys. Rev. **D 49** (1994) 3283, arXiv:hep-ph/9311248.

[37] ATLAS Collaboration, JHEP **10** (2014) 096, arXiv:1407.0350 [hep-ex].

[38] M. Cacciari, G. P. Salam, and G. Soyez, JHEP063, arXiv:0802.1189 [hep-ph].

[39] M. Cacciari and G. P. Salam, Phys. Lett. **B 641** (2006) 57, arXiv:hep-ph/0512210 [hep-ph].

[40] C. G. Lester and D. J. Summers, Phys. Lett. **B463** (1999) 99–103, arXiv:hep-ph/9906349.

[41] A. J. Barr, C. G. Lester, and P. Stephens, J.Phys.G **G29** (2003) 2343–2363, arXiv:hep-ph/0304226.

[42] J. T. Linnemann, arXiv:physics:0312059.

[43] The ATLAS Collaboration, arXiv:0901.0512 [hep-ex] (2009).